



Contents lists available at ScienceDirect

## Journal of Physics and Chemistry of Solids

journal homepage: [www.elsevier.com/locate/jpcs](http://www.elsevier.com/locate/jpcs)Anisotropic scattering and superconductivity in high- $T_c$  cupratesM.M.J. French<sup>a</sup>, M. Abdel-Jawad<sup>a</sup>, J.G. Analytis<sup>a</sup>, L. Balicas<sup>b</sup>, N.E. Hussey<sup>a,\*</sup><sup>a</sup> H.H. Wills Physics Laboratory, University of Bristol, Bristol BS8 1TL, UK<sup>b</sup> National High Magnetic Field Laboratory, Florida State University, Tallahassee, FL 32306, USA

## ARTICLE INFO

PACS:  
74.72.Jt  
75.47.-m

## Keywords:

A. Superconductors  
D. Electrical conductivity  
D. Fermi surface  
D. Transport properties  
D. Superconductivity

## ABSTRACT

The isotropic and anisotropic components of the transport scattering rate in overdoped  $Tl_2Ba_2CuO_{6+\delta}$  are determined for a range of  $T_c$  values between 15 and 35 K by angle-dependent magnetoresistance measurements at  $T = 40$  K. The anisotropic scattering term is found to scale linearly with  $T_c$  and appears to vanish at the point where superconductivity is destroyed, establishing a clear link between the superconducting and normal state physics. Comparison with results from angle resolved photoemission spectroscopy suggests that the transport and quasi-particle lifetimes are very different.

Crown Copyright © 2008 Published by Elsevier Ltd. All rights reserved.

## 1. Introduction

Normal state transport properties of superconductors frequently serve as a useful guide to the nature of the electron pairing mechanism. In conventional superconductors, for example, the strength of the electron–phonon (e–ph) coupling is manifested in the magnitude of the normal state resistivity, or more specifically, the strength of the transport scattering rate  $1/\tau_{tr}$ . At elevated temperatures, where the resistivity is  $T$ -linear,  $1/\tau_{tr}$  is related to the e–ph coupling constant  $\lambda_{e-ph}$  via  $\hbar/\tau_{tr} = 2\pi k_B T_c \lambda_{e-ph}$  where  $T_c$  is the superconducting transition temperature.

In high temperature superconductors (HTSC), the doping dependence of the in-plane resistivity  $\rho_{ab}(T)$  is largely generic and appears tied to the  $T_c$  parabola (for a review see [1]), suggesting an intimate relation between the normal state scattering and superconductivity. At optimal doping, for example,  $\rho_{ab}$  is strictly  $T$ -linear [2] over a wide temperature range [3] whilst the Hall coefficient  $R_H$  has its strongest  $T$ -dependence [4]. Despite intense efforts, however, any direct correlation between superconductivity and  $1/\tau_{tr}$  has failed to materialize, largely due to difficulties in establishing the intrinsic  $T$ - and momentum-dependence of  $1/\tau_{tr}$  itself.

Progress on this front was made recently through developments in the analysis of angle-dependent magnetoresistance (ADMR) measurements on HTSC [5–7]. ADMR measurements, angular variations in the interlayer resistivity  $\rho_{\perp}$  at constant

temperature  $T$  and magnetic field  $H$  [8], have provided detailed information of the Fermi surface (FS) in a variety of layered metals [9–11]. By incorporating basal-plane anisotropy into the ADMR analysis, new information, namely the  $T$ - and momentum ( $\mathbf{k}$ -) dependence of the scattering rate  $\Gamma(T, \mathbf{k})$  could be extracted. Subsequent ADMR measurements on heavily overdoped (OD)  $Tl_2Ba_2CuO_{6+\delta}$  (Tl2201) revealed that  $\Gamma(T, \mathbf{k})$  consisted of two components, one isotropic and quadratic in  $T$ , the other anisotropic, maximal near the saddle points at  $(\pi, 0)$  and proportional to  $T$  [5]. Significantly, the deduced scattering rate could account for both  $\rho_{ab}(T)$  and  $R_H(T)$  in this compound.

In this report, ADMR measurements at  $T = 40$  K and  $\mu_0 H = 45$  T are compared for a number of OD Tl2201 crystals with differing  $T_c$  values between 15 and 35 K. The strength of the anisotropic scattering is found to scale linearly with  $T_c$ , *extrapolating to zero at the doping level where superconductivity vanishes*. This new correlation implies that it is the *anisotropic* scattering mechanism that is intimately related to the mechanism of HTSC. In marked contrast to what has been inferred for the quasi-particle lifetime from angle resolved photoemission spectroscopy (ARPES) [12,13], no sign reversal of the anisotropy is observed. Finally, our results shed new light on the doping evolution of both  $\rho_{ab}(T)$  and  $R_H(T)$  in OD cuprates.

## 2. Experimental method and results

A total of six self-flux grown  $\rho_{\perp}$  crystals [14] (typical dimensions  $0.3 \times 0.3 \times 0.03$  mm<sup>3</sup>) were annealed at temperatures  $300^\circ\text{C} \leq T \leq 600^\circ\text{C}$  in flowing  $O_2$  and mounted in a  $c$ -axis quasi-Montgomery configuration. ADMR were measured on a two-axis

\* Corresponding author. Tel.: +44 1179288140.  
E-mail address: [n.e.hussey@bristol.ac.uk](mailto:n.e.hussey@bristol.ac.uk) (N.E. Hussey).

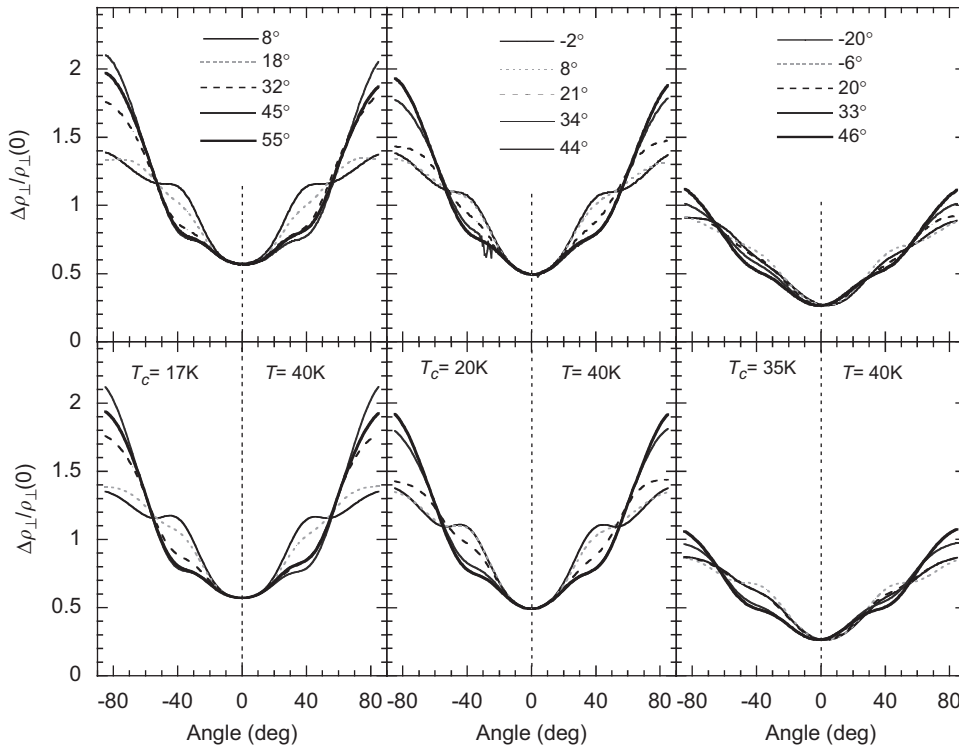


**Fig. 1.** Top panels: angle-dependent magnetoresistance sweeps for three different samples of overdoped TI2201 with  $T_c$  of 17 K (TI17K—left panel), 20 K (TI20K—middle panel) and 35 K (TI35K—right side) measured at 40 K and 45 T. Bottom panels: the least-square fits to each data set, respectively. The asymmetry around  $\theta = 0$  arises from slight misalignment of the crystalline  $c$ -axis with respect to the rotational platform. The inclusion of a coordinate axis rotated with respect to the platform axis can account for such a distortion and has been added to our fitting routine. This correction, however, has a negligible effect on the parameters obtained.

rotator in the 45 T hybrid magnet at the NHMFL in Florida using a conventional four-probe ac lock-in technique. The orientation of the crystal faces was indexed for a number of crystals using a single crystal X-ray diffractometer.

The top panels of Fig. 1 show polar ADMR data  $\Delta\rho_{\perp}/\rho_{\perp}(0)$  (normalized to their zero-field value) at different azimuthal angles  $\phi$  (relative to the Cu–O–Cu bond direction) for three crystals TI17K, TI20K and TI35K (the numbers relate to their  $T_c$  values). Similar data for the other three crystals measured in this study (TI15Ka, TI15Kb and TI32K) have already been published elsewhere [5,15]. Note that  $\Delta\rho_{\perp}/\rho_{\perp}(0)$  is significantly larger for the lower  $T_c$  crystals. Moreover, near  $\mathbf{H}_{\parallel c}$  ( $\theta = 0$ ), the TI35K curves are more V-shaped than rounded. As shown below, these features are caused by the higher  $T_c$ , less OD samples possessing a significantly larger relative basal-plane anisotropy in  $\omega_c\tau$ , the product of the cyclotron frequency and the transport lifetime [5].

In order to extract information on the FS and  $\omega_c\tau$ , we carried out a least-square fitting of the data using the Shockley–Chambers tube integral form of the Boltzmann transport equation modified for a quasi-2D metal with a four-fold anisotropic scattering rate  $1/\tau(\varphi) = (1 + \alpha \cos 4\varphi)/\tau^0$  and anisotropic in-plane velocity  $v_F(\varphi)$ , incorporated via  $1/\omega_c(\varphi) = (1 + \beta \cos 4\varphi)/\omega_c^0$  [5,6]. The sign of  $\alpha$  defines the azimuthal location of maximal scattering. The FS wavevector  $k_F(\theta, \varphi)$  was parameterized into lowest order harmonic components satisfying the body-centered tetragonal symmetry of TI2201 [16]:

$$k_F(\theta, \varphi) = k_{00} - k_{40} \cos 4\varphi - k_{21} \cos(k_z c/2) \sin 2\varphi - k_{61} \cos(k_z c/2) \sin 6\varphi - k_{101} \cos(k_z c/2) \sin 10\varphi \quad (1)$$

where  $k_z$  is the  $c$ -axis wavevector and  $c$  is the interlayer spacing. Note that  $k_{21}$ ,  $k_{61}$  and  $k_{101}$  are small compared to  $k_{00}$ , the radius of

the cylindrical FS (about the zone corners), and  $k_{40}$ , its in-plane squareness, and only their ratio (e.g.  $k_{61}/k_{21}$ ) can be determined to good accuracy. To minimize the number of free parameters, we fix  $k_{101}/k_{21} = k_{61}/k_{21} - 1$  such that  $t_{\perp}(\varphi)$  vanishes at both the nodes and the anti-nodes [11,17] and fix  $k_{00}$  using the empirical relation  $T_c/T_c^{\max} = 1 - 82.6(p - 0.16)^2$  with  $T_c^{\max} = 92$  K and  $(\pi k_{00}^2)/(2\pi/a)^2 = (1 + p)/2$  [18]. The coefficient  $\beta$  depends largely on our choice of  $k_{61}/k_{21}$  with the best least-square ( $\chi^2$ ) values giving  $\beta = 0 \pm 0.1$  for  $0.6 \leq k_{61}/k_{21} \leq 0.8$  for all samples. The sum  $\alpha + \beta$  was much less sensitive to variations in  $k_{61}/k_{21}$ , however, and for simplicity, we assume hereafter  $\omega_c(\varphi) = \omega_c^0$ .

The best fits, shown in the bottom panels of Fig. 1, are all excellent and the four remaining fitting parameters (see Ref. [15]) are well constrained due to the wide range of polar and azimuthal angles studied. Within our experimental resolution, the FS parameters appear to have negligible doping dependence. Moreover, the projected in-plane FS is found to be in good agreement with recent ARPES measurements on the same compound [13]. The anisotropy parameter  $\alpha$  increases with rising  $T_c$  whilst  $\omega_c^0\tau^0$  shows the opposite trend (as is evident from the overall reduction in the ADMR signal in Fig. 1).

### 3. Discussion and analysis

Our previous  $T$ -dependent analysis of TI15Ka implied the presence of two inelastic scattering channels in the current response of OD TI2201 [5]. Accordingly we split  $1/\omega_c^0\tau(\varphi)$  into isotropic and anisotropic components  $\gamma_{\text{iso}} = (1 - \alpha)/\omega_c^0\tau^0$  and  $\gamma_{\text{aniso}} = 2\alpha/\omega_c^0\tau^0 \cos^2 2\varphi$ . In TI15Ka,  $\gamma_{\text{iso}} \sim A + BT^2$ , reflecting a combination of impurity and electron–electron scattering, whilst  $\gamma_{\text{aniso}} \sim CT$  [5], the microscopic origin of which has yet to be identified. The doping ( $T_c$ ) dependence of  $\gamma_{\text{iso}}$  and  $\gamma_{\text{aniso}}$

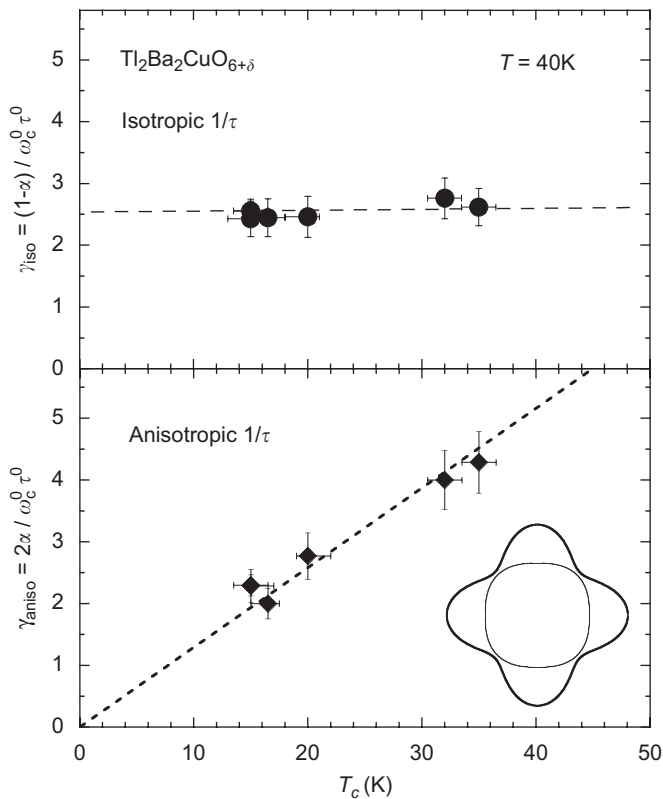


**Fig. 2.** (Top) Doping dependence of  $\gamma_{\text{iso}} \equiv (1 - \alpha)/\omega_c^0 \tau^0$  at  $T = 40\text{K}$ . (Bottom) Doping dependence of  $\gamma_{\text{aniso}} \equiv 2\alpha/\omega_c^0 \tau^0$  (diamonds) at  $T = 40\text{K}$ . Azimuthal variation of  $\gamma_{\text{aniso}}$  (solid line) with respect to  $k_F(\varphi)$  (thin line) is illustrated as an inset.

(at  $T = 40\text{K}$ ) are shown in the top and bottom panels of Fig. 2, respectively.  $\gamma_{\text{iso}}$  exhibits very little change with doping, indicating that both impurity and electron–electron scattering are relatively constant over this narrow composition range. The more striking result is the doping dependence of  $\gamma_{\text{aniso}}$  and in particular, the linear scaling of  $\gamma_{\text{aniso}}$  with  $T_c$  extrapolating to zero at the onset of superconductivity (on the OD side). Within a standard rigid band model, one would expect anisotropy in  $v_F(\varphi)$  and hence  $\omega_c(\varphi)$  to increase with doping as the FS at the Brillouin zone boundary approaches the saddle points. The fact that the data show the opposite trend is therefore significant and justifies our key assumption that the basal-plane anisotropy found in Tl2201 is dominated by anisotropy in  $1/\tau(\varphi)$  which surprisingly for such highly OD samples remains significant (the absolute anisotropy  $\gamma(\pi, 0)/\gamma(\pi, \pi) \sim 3$  for Tl40K at  $T = 40\text{K}$ ).

This empirical correlation between  $\gamma_{\text{aniso}}$  and  $T_c$  has several implications for the normal state of OD cuprates. Firstly, given that the carrier concentration is varying only weakly (as  $1 + p$ ) in this doping range, it is apparent that the marked change in the absolute value of resistivity with doping [14,19] is due primarily to a decrease in anisotropic scattering. Secondly, the preservation (at the Fermi level) of the full FS volume implies that there is no pseudogap in OD Tl2201 for  $x \geq 0.24$ , as argued by Tallon and Loram [20]. Whilst one might argue that such a large applied field could suppress any pseudogapping in our crystals [21], our conclusion is consistent with the observation of metallic zero-field  $\rho_c(T)$  at all finite temperatures. The  $c$ -axis pseudogap, inferred from interlayer tunnelling measurements [21] and scanning tunnelling microscopy (STM) [22] on  $\text{Bi}_2\text{Sr}_2\text{CaCu}_2\text{O}_{8+\delta}$ , is therefore a non-universal feature of OD cuprates.

Lastly and most importantly, the suppression of superconductivity on the OD side looks to coincide with the disappearance

of (the  $T$ -linear)  $\gamma_{\text{aniso}}$ . This conclusion is consistent with the observation of a strictly  $T^2$  resistivity in heavily OD, non-superconducting  $\text{La}_{1.7}\text{Sr}_{0.3}\text{CuO}_4$  below  $50\text{K}$  [23] and indicates an intimate relation between the anisotropic scattering and HTSC. Our findings contrast markedly with the doping evolution of the imaginary part of the quasi-particle self-energy  $\text{Im}\Sigma$  inferred from ARPES. Here the nodal/antinodal quasi-particle anisotropy is seen to vanish [24] or even reverse its sign [12,13] before superconductivity is suppressed on the OD side. ARPES-specific issues such as resolution, background subtraction and matrix-element effects are not believed to be important here [25]. One thus needs to ask the question whether the two probes are in fact measuring a similar quantity. Direct comparison of the scattering rates deduced from AMRO (this study and Ref. [26]) and ARPES [13] in Tl2201 ( $T_c \sim 30\text{K}$ ) shows that the former is one order of magnitude smaller. Given that AMRO is a bulk transport probe, the anomalously large linewidths seen in ARPES most likely result from additional (small-angle) scattering due to surface or single-particle effects though more systematic studies are clearly required to elucidate this discrepancy.

As stated above,  $\gamma_{\text{aniso}}(T)$  could account for both  $R_H(T)$  and  $\rho_{ab}(T)$  in Tl15Ka at low  $T$  [5]. To simulate the doping evolution of  $\rho_{ab}(T, p)$  and  $R_H(T, p)$  in Tl2201, we adopt a simple one-parameter scaling model and calculate  $\rho_{ab}(T, p)$  and  $R_H(T, p)$  using the Jones–Zener expansion of the linearized Boltzmann transport equation for a quasi-2D FS [27]. Firstly,  $k_{40}$  and  $k_{00}$  are fixed using the values for Tl15Ka ( $= 0.034$  and  $0.73\text{Å}^{-1}$ , respectively, [15]) and the scaling relation [18] described earlier. Secondly,  $1/\omega_c \tau$  is expressed as  $\gamma(T, \varphi) = \gamma_{\text{iso}}(T) + \gamma_{\text{aniso}}(T, \varphi) = A + BT^2 + C(p)T \cos^2 2\varphi$  where  $C(p) = C(\text{Tl15Ka}) \times T_c(p)/15$ . Finally, the anticipated return to isotropic scattering at high  $T$  is simulated by inclusion (in parallel) of a maximum scattering rate  $\Gamma_{\text{max}} = \langle v_F(\varphi) \rangle / a$  in accord with the Mott–Ioffe–Regel limit [28]. In this way,  $\gamma(T, \varphi)$  saturates at different points on the FS at different  $T$  [27] or  $\omega$  [29]. Indeed, anisotropy in the onset of saturation of  $\text{Im}\Sigma(\omega)$  was recently observed in optimally doped  $\text{La}_{2-x}\text{Sr}_x\text{CuO}_4$  [30].

The resultant simulations for both  $R_H(T, p)$  and  $\rho_{ab}(T, p)$  are presented in Figs. 3 and 4, respectively, for  $T_c = 0, 30, 60$  and  $90\text{K}$ . Despite the one-parameter ( $= C(p)$ ) scaling, the  $R_H(T)$  plots show very reasonable qualitative and quantitative agreement with experimental data (shown as solid symbols) [19,26]. The  $p$ -dependence of  $\rho_{ab}(T)$  also agrees reasonably well with

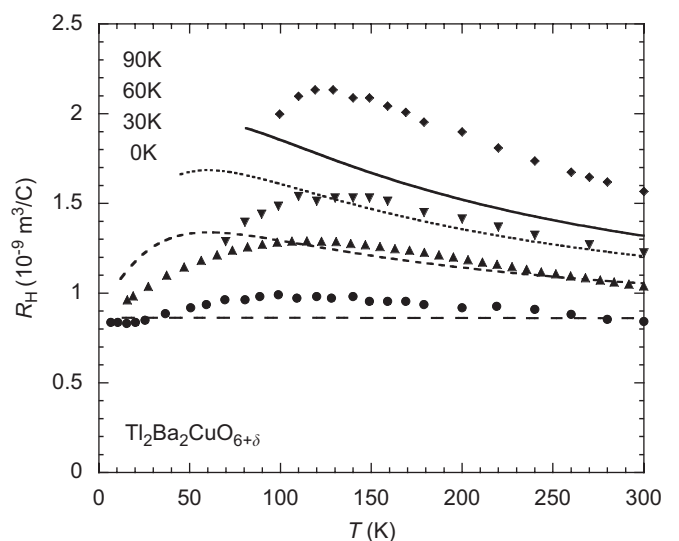


**Fig. 3.** Simulations of  $R_H(T)$  for Tl2201 with  $T_c$  values of 0, 30, 60 and  $90\text{K}$  (solid lines) together with data for  $T_c$  values  $< 4\text{K}$  (circles, [19]),  $25\text{K}$  (triangles, [26]),  $62\text{K}$  (inverted triangles, [19]) and  $81\text{K}$  (diamonds, [19]).

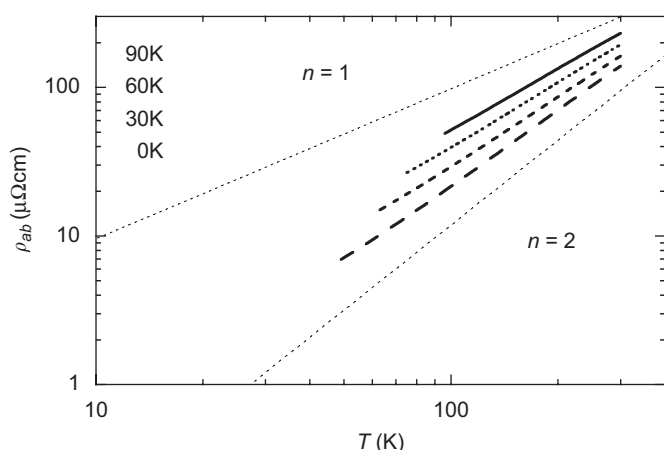


**Fig. 4.** Simulation of  $\rho_{ab}(T) - \rho_{ab}(T=0)$  (on a log-log scale) for Tl2201 with  $T_c$  values of 0, 30, 60 and 90 K (solid lines) using the same parameterization.

experiment, where the exponent  $n$  of  $\rho_{ab}$  is found to evolve smoothly from 1 to 2 between optimal doping and the SC/non-SC boundary (not shown for clarity) [19]. (The in-plane magnetoresistance  $\Delta\rho_{ab}/\rho_{ab}$  is also seen to have the correct magnitude and  $T$ -dependence [15,26].) This correspondence, plus the fact that our simulations could track the marked increase in the magnitude of  $R_H$  for what are relatively small changes in carrier concentration, suggests that anisotropic scattering is indeed the source of the  $T$ - and  $p$ -dependence of  $R_H$  across the OD regime. This monotonic variation of  $R_H$  with doping, however, is incompatible with the sign reversal of the scattering rate anisotropy inferred from ARPES [12,13].

Finally, let us briefly examine possible origins for the observed anisotropy. Real-space (correlated) electronic inhomogeneity, as reported in recent STM studies [31], is one possible candidate though as yet, no measurements have been performed on heavily OD non-SC cuprates to establish any possible link between inhomogeneity and superconductivity. Interactions with a bosonic mode are another possibility, though given the strong angle and doping dependence, presumably not phonons. More likely candidates include spin, charge (stripe) or  $d$ -wave pairing fluctuations which all disappear with superconductivity on the OD side [32–34]. The preservation of the  $T$ -linear scattering rate to low  $T$ , however, implies a vanishingly small energy scale for these fluctuations, characteristic of proximity to a quantum critical point. Intriguingly, Dell'Anna and Metzner recently calculated the transport scattering rate close to a 2D Pomeranchuk instability that is identical in form to the one observed in OD Tl2201 [35] though how scattering intensity *diminishes* with doping within this scenario as one approaches the van Hove singularity remains to be clarified.

## 4. Conclusions

In conclusion, we have formulated a clear correlation between  $T_c$  and a normal state property in cuprates, specifically the anisotropy of the transport scattering rate. Although this study is necessarily focused on heavily OD cuprates, it has implications for the entire phase diagram, in particular the evolution of  $R_H(T, p)$ . In addition, the present results support a previously unforeseen link between the normal state scattering and superconducting mechanisms. Finally, our AMRO results affirm that maximal scattering remains at the antinodes throughout the OD region, in contrast to what has been recently inferred from ARPES measurements of the quasi-particle lineshape.

## Acknowledgments

We thank A. Carrington and J.P.H. Charmant for technical assistance and A. Damascelli, M.P. Kennett, R.H. McKenzie and J.A. Wilson for helpful discussions. This work was supported by EPSRC and a co-operative agreement between the State of Florida and NSF.

## References

- [1] N.E. Hussey, J. Phys.: Condens. Matter 20 123201 (2008).
- [2] Y. Ando, et al., Phys. Rev. Lett. 93 (2004) 267001.
- [3] M. Gurvitch, A.T. Fiory, Phys. Rev. Lett. 59 (1987) 1337.
- [4] H.Y. Hwang, et al., Phys. Rev. Lett. 72 (1994) 2636.
- [5] M. Abdel-Jawad, et al., Nat. Phys. (London) 2 (2006) 821.
- [6] M.P. Kennett, R.H. McKenzie, Phys. Rev. B 76 (2007) 054515.
- [7] J.G. Analytis, et al., Phys. Rev. B 76 (2007) 104523.
- [8] K. Yamaji, J. Phys. Soc. Jpn. 58 (1989) 1520.
- [9] M.V. Kartsovnik, Chem. Rev. 104 (2004) 5737.
- [10] L. Balicas, et al., Phys. Rev. Lett. 94 (2005) 236402.
- [11] N.E. Hussey, et al., Nature (London) 425 (2003) 814.
- [12] X.J. Zhou, et al., Phys. Rev. Lett. 92 (2004) 187001.
- [13] M. Platé, et al., Phys. Rev. Lett. 95 (2005) 077001.
- [14] A.W. Tyler, D.Phil. Thesis, Cambridge University, 1998.
- [15] M. Abdel-Jawad, et al., Phys. Rev. Lett. 99 (2007) 107002.
- [16] C. Bergemann, et al., Adv. Phys. 52 (2003) 639.
- [17] O.K. Andersen, et al., J. Phys. Chem. Solids 56 (1995) 1573.
- [18] M.R. Presland, et al., Physica (Amsterdam) 176C (1991) 95.
- [19] Y. Kubo, et al., Phys. Rev. B 43 (1991) 7875.
- [20] J.L. Tallon, J.W. Loram, Physica (Amsterdam) 349C (2001) 53.
- [21] T. Shibauchi, et al., Phys. Rev. Lett. 86 (2001) 5763.
- [22] C. Renner, et al., Phys. Rev. Lett. 80 (1998) 149.
- [23] S. Nakamae, et al., Phys. Rev. B 68 (2003) 100502.
- [24] K. Yang, et al., Phys. Rev. B 73 (2006) 144507.
- [25] D.C. Peets, et al., cond-mat/0609250.
- [26] N.E. Hussey, et al., Phys. Rev. Lett. 76 (1996) 122.
- [27] N.E. Hussey, Eur. Phys. J. B 31 (2003) 495.
- [28] N.E. Hussey, K. Takenaka, H. Takagi, Philos. Mag. 84 (2004) 2847.
- [29] N.E. Hussey, J.C. Alexander, R.A. Cooper, Phys. Rev. B 74 (2006) 214508.
- [30] J. Chang, et al., Phys. Rev. B 75 (2007) 224508.
- [31] K. McElroy, et al., Phys. Rev. Lett. 94 (2005) 197005.
- [32] L.B. Ioffe, A.J. Millis, Phys. Rev. B 58 (1998) 11631.
- [33] S. Wakimoto, et al., Phys. Rev. Lett. 92 (2004) 217004.
- [34] D. Reznik, et al., Nature (London) 440 (2006) 1170.
- [35] L. Dell'Anna, W. Metzner, Phys. Rev. Lett. 98 (2007) 136402.